CHARACTERIZING THE DROUGHT DEVELOPMENT IN THE PHILIPPINES USING MULTIPLE DROUGHT INDICES DURING THE 2019 EL NIÑO

Gay Jane Perez[a,b]*, Odette Enricuso[b], Kimberly Manauis[a], Michael Angelo Valete[a]

[a]Institute of Environmental Science and Meteorology, University of the Philippines Diliman, Quezon City, 1101, Philippines - gpperez1@up.edu.ph, kamanauis@up.edu.ph, mpvalete@up.edu.ph,
[b]Philippine Space Agency, Quezon City, 1101, Philippines - gay.perez@philsa.gov.ph, odette.enricuso@philsa.gov.ph

KEY WORDS: El Niño, yield loss, agricultural drought, drought index, MODIS, TRMM.

ABSTRACT:

Drought events in the Philippines have resulted in a significant loss in crop production. This study investigated the drought development during the 2019 weak El Niño using different drought indices at a country and local scale. Satellite data from MODIS were used to derive Normalized Difference Vegetation Index (NDVI) anomaly, Vegetation Health Index (VHI), and Standardized Vegetation and Temperature Ratio (SVTR), while TRMM was used for the Standardized Precipitation Index (SPI). These indices were compared with crop production data at national scale and crop damage reports at local scale. The results showed consistency in the spatiotemporal variation of drought events, where drought peak occurred during March to April in most indices and indicators. Based on the values of SPI, the areas with rainfall deficit increased from January to April (25% to almost 100%), but looking at vegetation stress, around 50% was affected, as seen by SVTR and VHI. Yield loss during the first and second quarter after the El Niño peak increased up to 20%, especially in the western region in the Philippines. Overall findings demonstrate the relevance of utilizing multiple drought indices and indicators that characterize drought evolution, from drought onset to the peak of agricultural drought, which is essential in developing a robust drought metric for the Philippines.

1. INTRODUCTION

In the last few decades, the trend in Philippine crop production has increased through improved practices in agriculture and genetics (Branca et al., 2011). Investments in yield and acreage are owed to innovations in agricultural practices, increasing the rice production from ∼3.9 million tonnes in 1961 to ∼19.0 million tonnes in 2018 (FAOSTAT, 2020). However, this upward trend has been interrupted with episodes of drought where severe events are often associated with El Niño (Stuecker et al., 2018). From 2015 to 2019, two El Niño episodes with different magnitudes (weak and strong) have impacted the country's agricultural sector, which resulted in an approximately USD 157 and 327 million worth of crop damages, respectively. Severe droughts in the Philippines prompted drought mitigation measures such as the formation of the El Niño Task Force and the drought advisories issued by the Department of Science Technology - Philippine Atmospheric, Geophysical and Astronomical Services Administration (DOST-PAGASA), the weather bureau of the country, as a directive to monitor the phenomenon closely (Urich et al., 2009). These advisories are primarily based on ground-derived rainfall data and do not include variables important to agriculture such as vegetation health and temperature.

Drought usually begins with precipitation deficit (also known as meteorological drought) then leads to soil moisture deficit and higher land surface temperature, which eventually affects vegetation growth (also known as agricultural drought) (Gillette, 1950). It is then critical to consider the spatiotemporal dynamics of different key drought-related variables to understand drought propagation especially in vulnerable agricultural areas. Concurrent with the advances in remote sensing, drought monitoring approaches began maximizing satellite-derived variables, such as rainfall, Land Surface Temperature (LST), and Normalized Difference Vegetation Index (NDVI) to derive drought indicators and indices. Anomalous behaviour of these variables indicates early stages of dry conditions and vegetation stress.

Several studies have developed drought indices and examined their capabilities in monitoring and characterizing agricultural drought, where rainfall was solely used as an early indicator (McKee et al., 1993) while NDVI and LST were used to represent soil moisture stress. Kogan et al. (1990) developed the Vegetation Health Index (VHI) using NDVI and LST data to measure drought intensity and duration across locations. Due to the sensitivity of VHI with precipitation and temperature variations, it can be used in developing a comprehensive, crop-specific index such as Agricultural Stress Index (ASI) in which it integrates the spatial and temporal dimensions of VHI coupled with crop coefficients as input parameters (Rojas, 2020). On the other hand, a localized agricultural drought index was developed and tested during the 2015-2016 drought in the Philippines (Perez et al., 2016). The study showed that the Standardized Vegetation Temperature Ratio (SVTR), with similar parameters such as in VHI, was able to detect below-normal rice yields across different climate types in the country.

To the author's knowledge, there has not been a comprehensive study that utilizes well-established drought indices in characterizing drought development in the country. This study aims to describe the drought development in the country during the 2019 weak El Niño using multiple drought indices, namely NDVI, SPI, VHI, and SVTR during and after the El Niño period at a country and local scale. At the country scale assessment, spatiotemporal dynamics of drought indicators and indices were investigated through time series analysis. Moreover, drought development was further assessed in a drought-affected region of Occidental Mindoro against rice and corn crop damages

* Corresponding author

from provincial records. In this study, the authors acknowledge the limitation of only looking at a single drought event using moderate satellite resolution products at monthly observations, which limits the detailed variation of the vegetation condition during a drought event. However, the investigation adds value in understanding drought propagation in the Philippines, as drought vulnerable regions are determined and studied. The study also emphasizes the importance of available corresponding ground data that permits the monitoring of drought at a local scale.

2. MATERIALS AND METHODS

Drought assessment in the Philippines was conducted within August 2018 to September 2019, which covers the months under El Niño (Figure 1) and the period after the event. The Oceanic Niño Index (ONI) is the three-month running mean of sea surface temperature anomalies in the Niño 3.4 region. An El Niño event is declared when ONI reaches 0.5°C or above for five consecutive months. In late 2018, ONI values went up to 0.7°C starting October, peaked at 0.9°C the following month and was consistent at 0.8°C for four consecutive months until it dropped to 0.3°C in July 2019, which depicts the termination of El Niño.

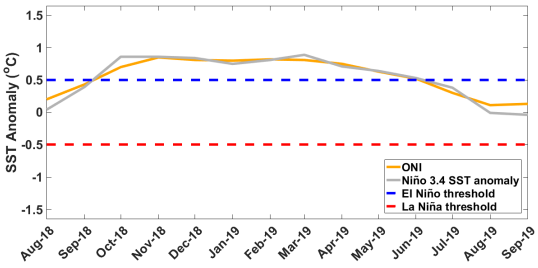

Figure 1. The ERSST v5 and ONI timeseries and the threshold for identifying ENSO events.

To assess the effects of El Niño in the Philippines, two levels of investigation were conducted, country scale and local scale, with further validation at the farm-level. The first assessment was used to determine the spatiotemporal evolution of drought. The second part of the evaluation focused on a drought-affected region, utilizing provincial crop damage reports to compare consistency in drought spatial patterns.

2.1 Data Acquisition and Processing

2.1.1 Geophysical Variables: The remotely sensed NDVI and LST products used for index derivation are from Moderate Resolution Imaging Spectroradiometer (MODIS) on board Terra satellite. MOD13C2 and MOD11C3 which are the monthly NDVI and LST, respectively, were downloaded from Land Processes Distributed Active Archive (LPDAAC) data pool. Quality assurance for MODIS NDVI and LST were applied. Rainfall data were acquired from Tropical Rainfall Measuring Mission (TRMM) satellite. The hourly rainfall rates were transformed to monthly rainfall. The product used to derive SPI and rainfall anomaly was the TRMM 3B43 v7. The pixel-wise NDVI, LST, and precipitation anomalies were computed using the average values of the dataset. Summarized in Table 1 are the satellite products used to derive the drought indices. All these global dataset layers were subset into the area of the Philippines (4.55°N - 21.28°N; 115.5°E - 126.93°E).

Parameters	Data Range	Sensor	Resolution
Rainfall	Jan 1998 to Sep 2019	TRMM	25 km
Land Surface Temperature	Feb 2000 to Sep 2019	MODIS	5 km
Normalized Difference Vegetation Index	Feb 2000 to Sep 2019	MODIS	5 km

Table 1. Drought parameters used in the study.

2.1.2 Ancillary Data: Crop production data from the Philippine Statistics Authority (PSA) from the first to third quarter of 2019 were utilized to assess the impacts of drought in selected regions namely Isabela, Occidental Mindoro, Camarines Sur, Zamboanga del Sur, and Maguindanao (see Appendix A). At the local scale, crop damage reports of rice and corn in the province of Occidental Mindoro were obtained from the Office of the Provincial Agriculturist (OPag) for the period January to April 2019. These reports contain information such as area affected in hectares (ha), stage of crop development, and area of standing crop per municipality. The damage reports in hectares of rice and corn were combined and visualized per municipality in QGIS 3.8.

2.2 Drought Indices

2.2.1 Standardized Precipitation Index: In this study, 21 years' worth of TRMM data were used to derive SPI. Two SPI timescales, SPI-1 (for 1-month timescale) and SPI-3 (for 3-month timescale), were derived (Valete and Perez, 2019). Meteorological drought was represented through SPI-1, which measures the 1-month precipitation deviation from the mean. On the other hand, SPI-3 measures the deviation of 3-month precipitation total from the mean (McKee, 1995) which is related to agricultural drought. A drought event has its confirmation only when a series of continuously negative values of SPI reach the value of -1 or less (McKee et al., 1993). In deriving SPI, the precipitation total is fitted to the gamma function. This probability density function is then transformed to a Gaussian distribution which gives the SPI value for the timescale used. Table 2 shows the classification of SPI values wherein negative values indicate less than average precipitation.

2.2.2 Vegetation Health Index: VHI combines Temperature Condition Index (TCI) and Vegetation Condition Index (VCI). TCI exhibits variation in thermal condition (Equation 1), while VCI is a pixel-wise normalization of NDVI (Equation 2). The value for α in Equation 3, which pertains to the contribution of the two indices, was set to 0.5 assuming even contribution from both parameters (Kogan, 2000). VHI values imply overall vegetation health which is utilized in classifying drought severities as shown in Table 2. Drought is experienced in a region when VHI values are below 40 (Kogan, 1990).

$$TCI = \frac{LST_{max} - LST}{LST_{max} - LST_{min}} \quad (1)$$

$$VCI = \frac{NDVI - NDVI_{min}}{NDVI_{max} - NDVI_{min}} \quad (2)$$

$$VHI = \alpha \times VCI + (1 - \alpha) \times TCI \quad (3)$$

This contribution has been peer-reviewed. The double-blind peer-review was conducted on the basis of the full paper.
https://doi.org/10.5194/isprs-annals-V-3-2022-463-2022 | © Author(s) 2022. CC BY 4.0 License.

2.2.3 Standardized Vegetation Temperature Ratio: SVTR is defined as:

$$SVTR = \frac{R_i - \bar{R}_i}{\sigma_{R_i}}, \quad (4)$$

where:

R_i = ratio of Normalized Difference Vegetation Index (NDVI) and Land Surface Temperature (LST) for month i
$\bar{R}_i$ = historical mean of NDVI-LST ratio for month i
σ_{R_i} = standard deviation of NDVI-LST ratio for month i

SVTR follows the inverse relationship between LST and NDVI which indicates vegetation stress, thus the index can be used to assess agricultural drought conditions in the country, especially in low-lying areas where temperature is not a limiting factor. Classification of SVTR values are shown in Table 2 wherein SVTR $\leq$ - 0.5 are associated with drought conditions (Perez et al., 2016).

Classification	SPI	VHI	SVTR
Extreme	0 to -0.99	-	-
Severe	-1.00 to -1.49	≤ 10	$<$-2.01
Moderate	-1.50 to -1.99	10 to 20	-1.01 to -2.01
Mild	-2.00 and less	20 to 40	-0.50 to -1.01
Normal	-	≥ 40	$>$-0.50

Table 2. Drought classification based on SPI (McKee et al., 1993), VHI (Kogan, 1990), and SVTR values (Perez et al., 2016).

2.3 Data Analysis

Maps of the drought indicators and indices at a country scale were utilized to describe the spatial patterns of drought development across months. Only the period January to April 2019 were highlighted to focus on the peak of the El Niño event. Furthermore, time series analysis of the drought indicators and indices were also conducted to describe the drought development within the period of August 2018 to September 2019, which covers a one-year assessment of the drought development, pre-drought, during drought, and post-drought. Boxplots were utilized to summarize the distribution of index values at a national scale. A corresponding areal extent percentage was also computed to indicate the number of pixels under drought as indicated by the index thresholds (Equation 5).

$$ArealPercent(\%) = \frac{Numberofpixelsbelowthreshold}{Totalnumberoflandareapixels} * 100 \quad (5)$$

The same boxplot time series was employed at a local scale, where the development of drought was closely assessed, from its onset up to the termination. A drought intensity and density map of the drought-affected region of Mindoro was also produced to compare it with the accumulated rice and corn damage reports of the region, from January 2019 to April 2019. The drought intensity map shows the averaged index values within the period while the drought density map indicates the percentage of the number of pixels under drought within the period. The map was compared with the accumulated damaged reports to confirm consistency in spatial patterns of drought in the area. The damage reports were also visualized in a map, represented by the total damaged area expressed in hectares. Both information from rice and corn were combined to compare it with the satellite-derived drought indices. The computational analyses and plotting were run using the MATLAB software ver. R2019a and Google Earth Engine, while the post-processing of maps was conducted in QGIS 3.8.

3. RESULTS

3.1 Drought development at a country scale

Figure 2 depicts the spatiotemporal evolution in rainfall and LST during the drought episode in January to April 2019. Negative rainfall anomalies dominated the eastern part of the Philippines across all months, as shown in Figure 2a, signifying the effect of El Niño, which also coincided with the northeast monsoon season. Furthermore, the negative rainfall anomalies started in the central region of the Philippines in January, then further spread in the southern regions until it mostly dominated the northeast, central, and southern regions during February, the month when El Niño was declared in the Philippines by PAGASA. On the other hand, monthly positive LST anomalies started in the western regions during February to March and propagated in the central regions during April, as shown in Figure 2b.

To better characterize how drought evolved during this period, we analyzed maps of the different drought indices described earlier. Figure 3a shows that meteorological drought stress, as indicated by orange and red regions in the SPI-1 maps, peaks in February, and persists until March. Whereas for SPI-3, which is a proxy for agricultural drought, stress started to manifest in January, and intensified in March and April (Figure 3b). The occurrence of stress in January for SPI-3 could be attributed to the persisting rainfall deficits in the previous two months of November to December (data not shown).

For the NDVI-LST-based drought indices, it can be seen in Figure 4 that the NDVI anomaly, SVTR, and NDVI generally exhibit similar trends and spatiotemporal patterns. Interestingly, the monthly NDVI anomalies shown in Figure 4a followed a similar trend with temperature (Figure 2b), where drought stress is concentrated in the western and central regions in the country during the drought peak in April.

Compared with rainfall anomalies where drought signals peaked in February, both LST and NDVI anomalies reached their peak drought stress values around March and April. The monthly observations revealed that the impacts on vegetation were detected when stress still persisted during March and April. Similar, but more pronounced, drought signal patterns are exhibited by SVTR and VHI, as shown in Figures 4b and 4c, respectively. Persistent and severe drought can be seen in the western and eastern regions such as Occidental Mindoro and Camarines Sur, respectively, while in the north, the province of Isabela shows moderate to severe drought, and for the southern regions, Maguindanao and Zamboanga del Sur shows moderate drought signals (see Appendix A).

To gain more insights on the development of drought on a longer time-scale, a boxplot time series and corresponding areal percentage from August 2018 to September 2019 are plotted for the different drought indices, as shown in Figure 5. Within the one-year assessment, the rainfall-based indices, SPI-1 and

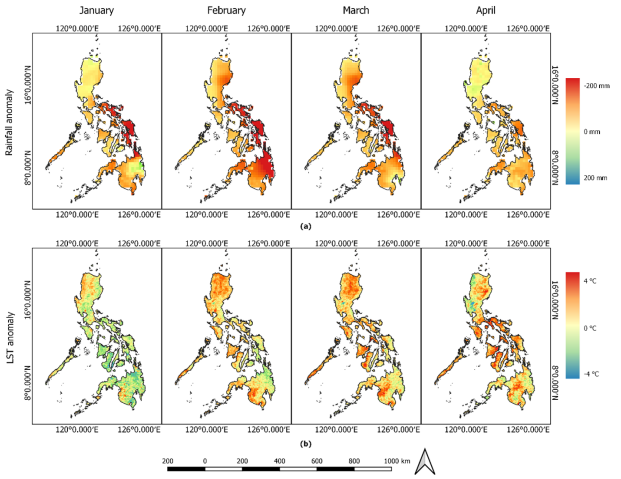

Figure 2. Monthly rainfall anomalies and the monthly land surface temperature anomalies derived from TRMM and MODIS, respectively.

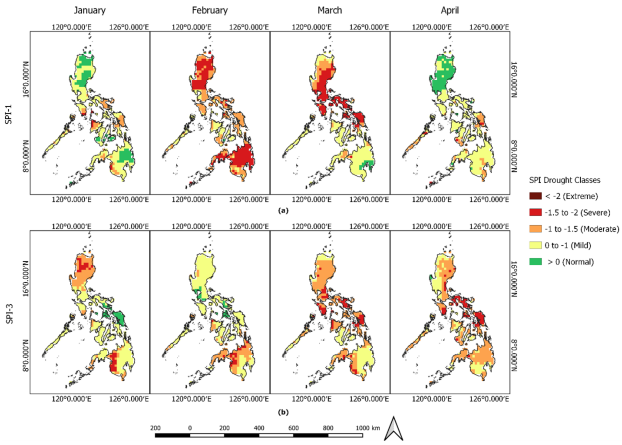

Figure 3. SPI at different timescales.

SPI-3 were already showing acute stress at the last quarter of 2018. In general, both indices already captured the effect of El Niño during this quarter where almost all regions of the country experienced rainfall deficits (Figure 5a and 5b). The tropical depression Usman that occurred in December and affected most of the southwestern regions of the country was reflected at the national scale, with more positive SPI values, indicating a temporary break from meteorological drought for SPI-1 but not with SPI-3 (Figure 5b). The narrow spread of the SPI-1 values during February (Figure 5a) further indicates the peak of meteorological drought, where most of the landmass of the country experienced mild to severe stress. The values started to increase in March until most of the values reached zero in July, signifying the dissipating signals of El Niño. In SPI-3 (Figure 5b), the spread of the values narrowed starting from November until its peak in April indicating the agricultural drought stress signals dominating the country. The negative values with much narrower spread were consistent from November to April. Notably, despite the consistent areal percentage from 80-100% of SPI-3, the distribution of the drought signals across the country started to decrease after the peak in April (Figure 5b).

On the other hand, NDVI anomaly, SVTR, and VHI showed similar trends when areal percentage is considered, but not

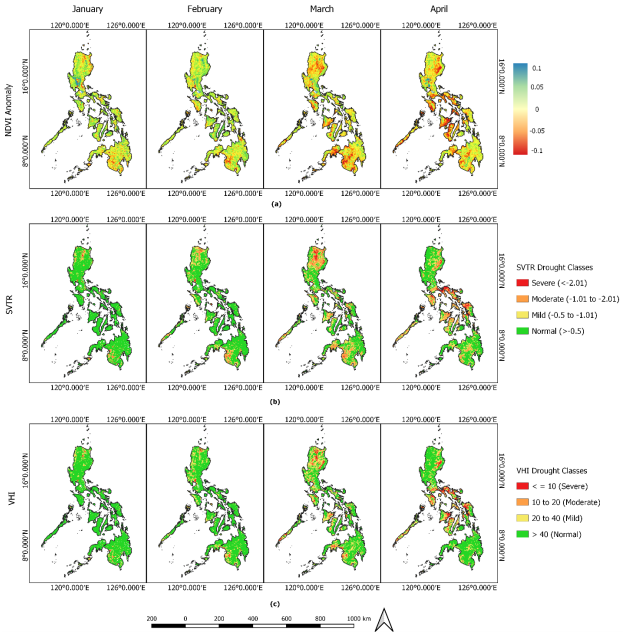

Figure 4. Monthly drought indices derived from MODIS product.

much information on spread can be observed from NDVI anomalies. It was only during March to April that the median values of the NDVI anomalies went below zero, indicating that the peak occurred during these months. For both SVTR and VHI, more noticeable patterns can be seen especially when looking at the drought affected areas at the national scale. The percentage of affected areas went beyond 50% in March to April but then eventually decreased in the following months. The boxplot was able to capture the difference in the spread of values of both indices, further signifying that both differ in indicating drought severity. Narrower spread of values of SVTR relative to VHI implies more drought signals identified in the country, especially in March, where most values reached the drought threshold in SVTR.

In looking at the areal percentage, the difference between rainfall-based indices and NDVI-LST based indices were highlighted. All land areas represented by pixels were under drought from February for SPI-1 (100%) while it was from March to April for SPI-3 (100%). This signifies that all land areas were identified to be in varying stress, from mild to severe, according to deviation in rainfall against the historical mean of 21 years. Similarly, SVTR and VHI had the highest number of affected land areas during March and April, from 41 to 48%, while it was 58% in April for NDVI anomalies. This indicates that the meteorological drought impact that propagated throughout the hydrological cycle only manifested in almost half of the landmass of the country, as identified by NDVI anomaly, SVTR, and VHI.

To assess the impacts of drought on crop production, data from Philippine Statistics Authority (PSA) were analyzed. The national crop production data showed a decrease in rice and corn yield gain by 4.44% and 6.14%, respectively, during the second quarter of 2019 compared to the previous year (PSA updated 2020). This decrease coincides with the peak of El Niño in 2019. Moreover, the majority of the drought hotspots mentioned above also incurred a decline in rice and corn yield gain by 1% to 20% and 0.1% to 26%, respectively, in the first to

third quarters of 2019 relative to 2018 (See Appendix B). This demonstrates the general agreement between the drought indices and the crop production data in signifying drought impacts on crops. On the other hand, the drought hotspot region in Maguindanao experienced a crop yield increase by 19% to 45% from the 2018 crop production data. This suggests that the satellite-derived drought indices overestimated the drought signals in the area within the drought period.

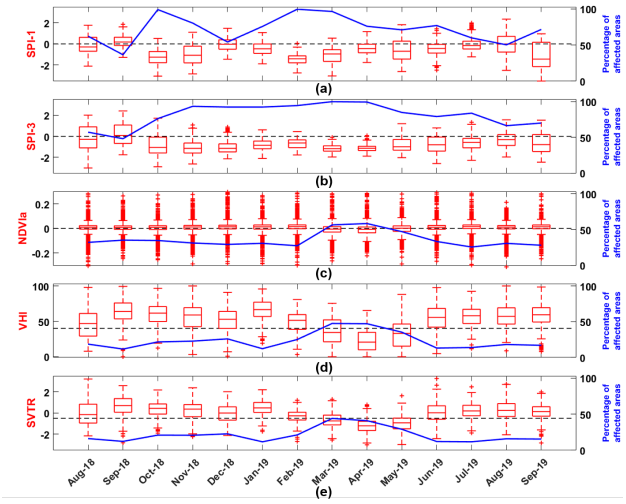

Figure 5. Boxplots of the drought indices within the 14-month period which includes the pre-drought, during drought, and post-drought events.

3.2 Drought development at a local scale

The development of drought was closely investigated in the drought-affected province of Occidental Mindoro (Figure 6). Compared to the national scale assessment, closer inspection at a drought-affected region revealed a clearer delineation of drought onset and termination. Values are much closer to each other, signifying the region to be dominated by drought signals. SPI-1 was used as an indicator for meteorological drought to determine drought onset and termination. SPI-1 identified two meteorological events in 2018 and 2019, as shown in Figure 6a. The first event started in August to November 2018 and terminated in December 2018, reflecting the impact of typhoon Usman at a regional scale. The second event covers the months from January to July 2019, which also coincided with the termination of El Niño according to ONI (Figure 1). For agricultural drought, SPI-3 identified one event from October 2018 up to July 2019 while for VHI and SVTR, both had similar duration from March to May 2019 (Figure 6d and Figure 6e). The differences of SPI-3 as a proxy for agricultural stress using rainfall only and SVTR and VHI as soil moisture proxy can be seen in how they identify drought events. The persisting stress as identified by SPI-3 across the three-month accumulation was captured, therefore, declaring drought from October until the termination of the El Niño event, whereas for SVTR and VHI, the inverse relationship of NDVI and LST were intense during March to May. LST anomalies were intense during these months (Figure 2), implying its effect on drought development. For NDVI anomalies, the persistence of stress only manifested during April to May, which coincided with the peaks of other indices, however, this index was not very sensitive in capturing acute stress in the region, which could be attributed to the spatiotemporal limitation of the products used.

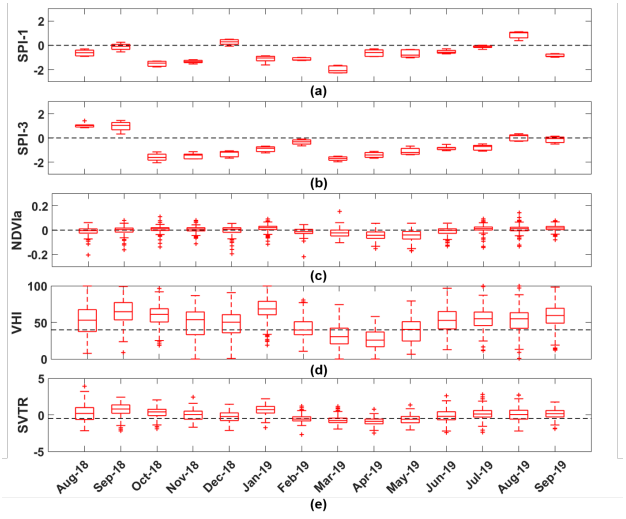

Figure 6. Drought temporal evolution in drought-affected province of Occidental Mindoro, as indicated by the boxplot time series of a) SPI-1, b) SPI-3, c) NDVIa, d) VHI, and e) VHI.

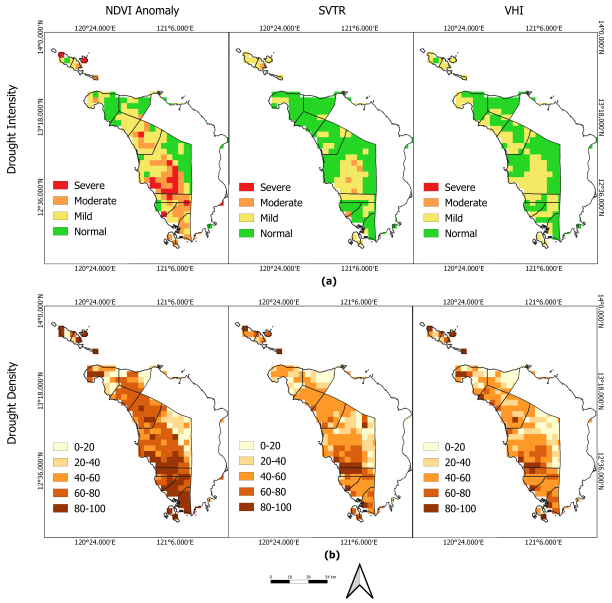

Figure 7. Drought intensity and density map of SVTR, VHI, NDVI anomaly.

The actual rice and corn damage reports (Figure 8) collected from the official provincial records of Occidental Mindoro were assessed with the drought indices, SVTR, VHI, and NDVI anomaly. This considered the accumulated reports within the growing season from January 2019 to April 2019. The drought intensity as an averaged index values from January to April 2019 period and the drought density (Figure 7), which indicates the frequency of each pixel under drought (VHI <40, SVTR $\leq$ -0.5, and NDVI anomaly <0), were compared with the aggregated rice and corn damaged areas to see spatial patterns of recurring drought and therefore, assess its consistency with the actual impacts.

SVTR and VHI captured more frequent drought pixels in the southern regions, while for NDVI anomaly, higher density can be found in most parts of the province (Figure 7a). For the

drought intensity, mild signals dominated the region as identified by both SVTR and VHI, while for NDVI anomaly, moderate and severe drought were also observed. Interestingly, NDVI anomaly and VHI were able to capture more drought signals in the central to southern regions of the province, which also reflected in the higher drought density in the area (Figure 7b).

In the actual crop damage reports for Occidental Mindoro (Figure 8), the southern regions incurred damages that were worth 1000 to 2000 hectares of farms. In addition, the northern region, particularly the municipality of Mamburao, incurred >500 hectares of damaged farms, while the rest of the municipalities declared damages <500 hectares only. Notably, the municipality of San Jose incurred the highest number of hectares damaged at >2000. This could be attributed to the occurrence of drought in the area during the younger stages of the crops, i.e. newly planted to vegetative, compared to other municipalities with affected crops only during its reproductive to mature stages, as reported by the provincial level crop damage records.

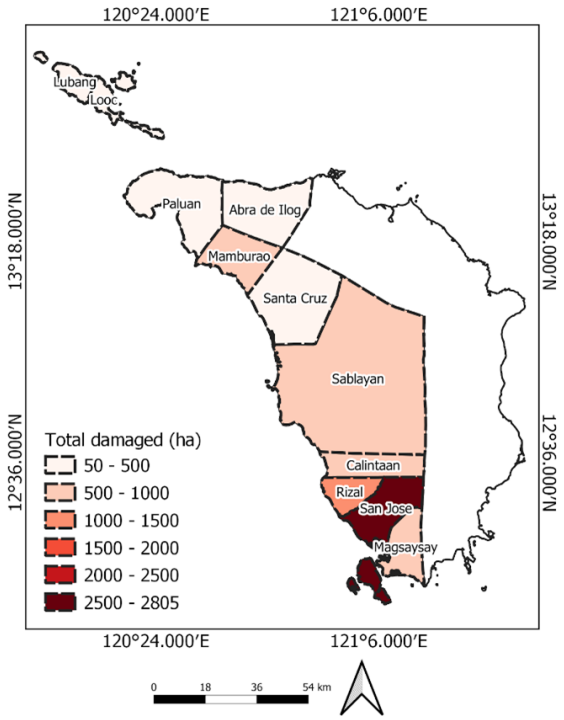

Figure 8. Crop damaged reports (rice and corn) expressed in total hectares damaged in Occidental Mindoro within the January to April 2019 cropping season.

4. DISCUSSION

The effects of El Niño such as the weaker monsoon activity and delayed onset of rainfall were reflected in the spatiotemporal dynamics of the drought indices and indicators utilized in the study. The weakened easterlies brought by El Niño is reflected in the negative rainfall anomalies that started in the eastern part of the country. The peak of the El Nino episode in February to March coincides with the dry months of the country, therefore, exacerbating dry conditions as seen in deficits in rainfall amount and hotter than normal temperatures.

Notably, areas with pronounced dry climate experienced positive temperature anomalies, which eventually spread in other parts of the country. In this case, drought propagation depends on the local climate type, where regions with distinct dry and wet seasons are more vulnerable to changes in monsoonal patterns. Recent insights on drought sensitivity highlighted the factors such as topography, climate, and soil characteristics, where areas with higher elevation, drier climate, and greater soil bulk density are more vulnerable to drought (Cartwright et al., 2020). Considering these different factors should reveal specific patterns of vulnerability that could be the basis for site- and crop-specific mitigation strategies in the drought hotspot regions.

The different stages of drought development were also identified based on different drought indicators and indices used in the study. At a country scale, rainfall deviations were prominent during February, whereas for NDVI and LST, its identified drought stress peaked one to two months after, from March to April. The same pattern was observed among drought indices, where agricultural drought indices, STVR, VHI, and SPI-3 were consistent with their identification of drought peak when compared with the meteorological drought index, SPI-1. The peak in drought values for SVTR and VHI only occurred later in March and April, which implies that despite the excess rainfall brought by Typhoon Usman in December, the persisting dry conditions brought by El Niño, impacted agriculture within one to two months after the temporary break from meteorological drought. The degree of moisture deficiency, as could be estimated from different SPI timescales, is an important factor to consider when anticipating drought impacts. In the study conducted in Indonesia, VHI was significantly correlated with SPI-3, indicating that rainfall deficit for three months has a significant impact on agricultural drought (Ma'Rufah et al., 2017). This further highlights the limitations and strengths of the different drought indicators and indices in characterizing different stages of the drought development. In this case, rainfall-based indices could be a suitable tool for drought propagation triggers but it is with temperature-vegetation based indices and other soil moisture-related indices that drought impacts on crops could be determined.

The 2019 weak El Niño started from October 2018 and ended in June 2019; however, its effects are still felt until September 2019. This has caused several drought events in the Philippines, as indicated by SPI, NDVI anomaly, VHI, and SVTR. SPI-1 identified two meteorological events, August 2018 to November 2018 and January 2019 to July 2019, separated by December 2018. SPI-1 values during December were higher than the threshold set for drought, which might be due to typhoon Usman bringing excess rainfall to most areas of the country during December 2018. For the agricultural drought indices, SPI-3 only started two months (October 2018) after SPI-1 identified meteorological drought, while for VHI and SVTR, it only started during March and extended up to April 2019. The growing season in most agricultural areas of the country starts from December to January, with the reproductive stages during March to April and harvesting around May. Despite a weak El Niño, the Philippines incurred billions of crop damages during this event, which could be attributed to the timing of the drought occurrence in the country. When drought impacts the water-demanding stage of the crop, i.e. vegetative to reproductive, this will affect the overall crop yield during the harvesting period. This was further demonstrated in the assessment of drought at a local scale. At the local scale, municipalities with younger crops at the time of the drought event incurred more damages relative to other regions with mature stages. Further-

This contribution has been peer-reviewed. The double-blind peer-review was conducted on the basis of the full paper.
https://doi.org/10.5194/isprs-annals-V-3-2022-463-2022 | © Author(s) 2022. CC BY 4.0 License.

more, when assessing the national crop yield data, decrease in crop yield mostly reflected during the second quarter of 2019, which is expected since most of the crops planted in the previous quarter coincided with the peak of El Niño. Drought hotspots identified by the satellite also incurred a decrease in crop yield which highlights the agreement between satellite estimation and crop production data, however, Maguindanao crop yield increased during this time period.

Results from this study demonstrate the relevance of utilizing multiple remotely sensed drought indices and indicators in characterizing the different stages of drought that have intensified to agricultural scales. The strength of the rainfall-based drought indices in indicating drought onset was highlighted in the study. At a different timescale such as SPI-3, drought persistence was captured and was consistent with the NDVI-based drought indices. However, the latter were more representative of the agricultural stress on the ground, as reflected in the spatial distribution of drought at a local scale. Overall, these indices look at different characteristics of drought, where one could indicate drought onset and termination and the other could indicate drought persistence. Their strengths in identifying specific drought characteristics could be combined to form a more robust drought metric. However, insights from the study also prompt the need to utilize spatiotemporally finer satellite data to be more efficient in representing farm-scale impacts and precisely discriminate different degrees of drought stress. An improved agricultural drought index would need further understanding on the relationship among the drought indicators and indices while considering the vegetation cover and anthropogenic influences in a specific location. Furthermore, verification studies using crop damage reports at a national scale highlights the importance of consistent and good quality data in the country.

5. CONCLUSION

Insights from the investigation on drought development during the 2019 weak El Niño in the Philippines revealed that the country is vulnerable to El Niño, especially distinctly drier regions in the western part of the country. Weak monsoonal activity in the east brought less rainfall and led to the drought propagation dominating the central region and the western areas where local climatic conditions have distinct wet and dry seasons, making these parts of the country drought hotspots regions. This also shows how drought development is a slow process, where different stages can be captured by different satellite-derived drought indicators and indices. In this study, these different tools were maximized to determine the early signs of drought stress, as can be seen using SPI-1, and to investigate the peak of agricultural drought using SPI-3, VHI, and SVTR. Meteorological drought index may have few direct impacts but it serves as an early indicator of drought, which is essential for drought mitigation measures. For SPI-3, VHI, and SVTR, their sensitivity to actual drought impacts are critical in risk assessment. For example, the decrease in crop yield at the first and second quarters of 2019 coincided with the drought peak identified by the drought indices, establishing the efficacy of satellite data to estimate impacts on crops.

Moreover, it was highlighted that drought impacts depend not only on severity but also on drought timing, as the peak of drought coincided with the sensitive stages of rice and corn farms in the drought-affected region of Mamburao, Occidental Mindoro, resulting in severe crop damages.

Overall, determining the strengths and limitations of each drought-related variable is essential in developing an integrated approach which could simultaneously detect multiple drought types. This will be key in developing an even more sensitive drought metric, as we aim to reduce uncertainties and increase accuracy of predictions to be more proactive in securing the food and water resources in the country. Findings from the study will be significant for the prioritization of drought assistance, especially in vulnerable regions, where drought conditions frequently develop.

ACKNOWLEDGEMENTS

This research was funded by the Department of Science and Technology - Philippine Council for Agriculture, Aquatic and Natural Resources Research and Development (DOST-PCAARRD). The authors would like to thank the Office of the Provincial Agriculture in Mamburao, Occidental Mindoro in helping during the drought validation in the municipality and providing the crop damage reports utilized in the study. Also, the authors would like to acknowledge Dr. Josefino Comiso for his inputs and guidance. Lastly, the support from the Drought and Crop Assessment and Forecasting (DCAF) Phase 2 project under the program Smarter Approaches to Reinvigorate Agriculture as an in Industry the Philippines (SARAI) Phase 2 funded by DOST-PCAARRD, with its co-implementing agencies, DOST-Philippine Atmospheric, Geophysical and Astronomical Services Administration (PAGASA) and Department of Agriculture- Bureau of Soils and Water Management (DA-BSWM), and members of Predictions of the Environment and Applications of Remote Sensing (PEARS) laboratory are acknowledged.

REFERENCES

Branca, G., McCarthy, N., Lipper, L., Jolejole, M. C., 2011. Climate-smart agriculture: a synthesis of empirical evidence of food security and mitigation benefits from improved cropland management. *Mitigation of climate change in agriculture series*, 3, 1–42.

Cartwright, J. M., Littlefield, C. E., Michalak, J. L., Lawler, J. J., Dobrowski, S. Z., 2020. Topographic, soil, and climate drivers of drought sensitivity in forests and shrublands of the Pacific Northwest, USA. *Scientific reports*, 10(1), 1–13.

FAOSTAT, 2020. *Food and Agriculture Organization of the United Nations*. http://www.fao.org/faostat/en/compare.

Gillette, H., 1950. A creeping drought under way. *Water and sewage works*, 104(5).

Kogan, F. N., 1990. Remote sensing of weather impacts on vegetation in non-homogeneous areas. *International Journal of remote sensing*, 11(8), 1405–1419.

Kogan, F. N., 2000. Satellite-observed sensitivity of world land ecosystems to El Nino/La Nina. *Remote Sensing of Environment*, 74(3), 445–462.

Ma'Rufah, U., Hidayat, R., Prasasti, I., 2017. Analysis of relationship between meteorological and agricultural drought using standardized precipitation index and vegetation health index. *IOP conference series: earth and environmental science*, 54number 1, IOP Publishing, 012008.

McKee, T. B., 1995. Drought monitoring with multiple time scales. *Proceedings of 9th Conference on Applied Climatology, Boston, 1995*.

McKee, T. B., Doesken, N. J., Kleist, J. et al., 1993. The relationship of drought frequency and duration to time scales. *Proceedings of the 8th Conference on Applied Climatology*, 17number 22, California, 179–183.

Perez, G., Macapagal, M., Olivares, R., Macapagal, E., Comiso, J., 2016. FORECASTING AND MONITORING AGRICULTURAL DROUGHT IN THE PHILIPPINES. *International Archives of the Photogrammetry, Remote Sensing & Spatial Information Sciences*, 41.

Rojas, O., 2020. Agricultural extreme drought assessment at global level using the FAO-Agricultural Stress Index System (ASIS). *Weather and Climate Extremes*, 27, 100184.

Stuecker, M. F., Tigchelaar, M., Kantar, M. B., 2018. Climate variability impacts on rice production in the Philippines. *PloS one*, 13(8), e0201426.

Urich, P. B., Quirog, L., Granert, W. G., 2009. El Nino: an adaptive response to build social and ecological resilience.

Valete, M. A., Perez, G. J., 2019. Evaluation of TRMM-based Standardized Precipitation Index for drought monitoring in the Philippines. *Proceedings of the Samahang Pisika ng Pilipinas*.

APPENDIX A

Selected drought hotspots in the Philippines within the 2019 El Niño Period

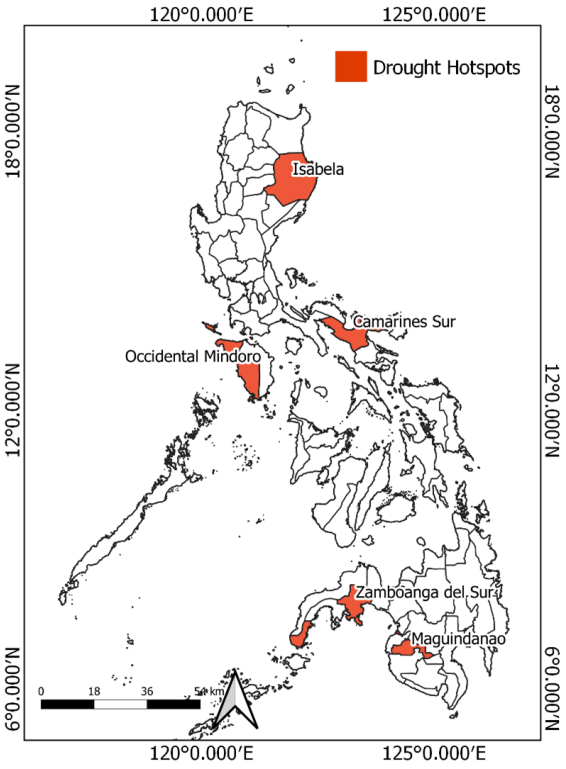

APPENDIX B

Percent of rice crop production yield gain in 2018 and 2019 for the whole Philippines and for selected provinces.

NATIONAL	% Rice Yield Gain 2018	% Rice Yield Gain 2018	% Loss
Quarter 1	9.73	8.62	-1.10
Quarter 2	10.60	6.16	-4.44
Quarter3	6.49	12.88	6.39
ISABELA			
Quarter 1	11.22	11.92	0.69
Quarter 2	11.57	10.38	-1.20
Quarter3	-1.55	15.73	17.29
OCCIDENTAL MINDORO			
Quarter 1	10.76	1.55	-9.22
Quarter 2	9.47	-10.63	-20.10
Quarter3	6.41	10.11	3.70
CAMARINES SUR			
Quarter 1	7.48	-4.34	-11.83
Quarter 2	10.21	-8.58	-18.79
Quarter3	9.89	7.04	-2.85
ZAMBOANGA DEL SUR			
Quarter 1	8.80	3.09	-5.71
Quarter 2	9.45	16.72	7.27
Quarter3	3.10	8.10	5.00
MAGUINDANAO			
Quarter 1	5.03	24.14	19.11
Quarter 2	0.18	26.20	26.02
Quarter3	-12.50	32.80	45.31